Supplementary Material to:

The first application of a numerically-exact, higher-order sensitivity analysis approach for atmospheric modelling: implementation of the hyperdual-step method in the Community Multiscale Air Quality Model (CMAQ) version 5.3.2

Jiachen Liu[1], Eric Chen[1], Shannon L. Capps[1]

[1]Department of Civil, Architectural & Environmental Engineering, Drexel University, Philadelphia, Pennsylvania, USA

Correspondence to: Shannon L. Capps (shannon.capps@drexel.edu)

1. Operations with hyperdual numbers

Examples of operations including addition, multiplication, exponential, natural log, power, and sine functions for hyperdual numbers $H_a = a_0 + a_1\epsilon_1 + a_2\epsilon_2 + a_{12}\epsilon_{12}$ and $H_b = b_0 + b_1\epsilon_1 + b_2\epsilon_2 + b_{12}\epsilon_{12}$ are listed in Eqs. S1-S6. These operations are derivations based on Fike and Alonso (2011).

$$H_a + H_b = a_0 + b_0 + (a_1 + b_1)\epsilon_1 + (a_2 + b_2)\epsilon_2 + (a_{12} + b_{12})\epsilon_{12} \tag{S1}$$

$$H_a H_b = a_0 b_0 + (a_1 b_0 + a_0 b_1)\epsilon_1 + (a_2 b_0 + a_0 b_2)\epsilon_2 + (a_0 b_{12} + a_1 b_2 + a_2 b_1 + a_{12} b_0)\epsilon_{12} \tag{S2}$$

$$\exp(H_a) = \exp(a_0) + [a_1 \exp(a_0)]\epsilon_1 + [a_2 \exp(a_0)]\epsilon_2 + [(a_1 a_2 + a_{12})\exp(a_0)]\epsilon_{12} \tag{S3}$$

$$\ln(H_a) = \ln(a_0) + \left(\frac{a_1}{a_0}\right)\epsilon_1 + \left(\frac{a_2}{a_0}\right)\epsilon_2 + \left(\frac{a_{12}}{a_0} - a_1 a_2\right)\epsilon_{12} \tag{S4}$$

$$H_a^{H_b} = \exp[H_b \ln(H_a)] \tag{S5}$$

$$\sin(H_a) = \sin(a_0) + [a_1 \cos(a_0)]\epsilon_1 + [a_2 \cos(a_0)]\epsilon_2 + [a_{12} \cos(a_0) - a_1 a_2 \sin(a_0)]\epsilon_{12} \tag{S6}$$

The power function (Eq. S5) is defined with both the natural log and exponential to avoid explicitly writing out the operations, which could be very complicated.

2. Slopes and R^2 values of additional one-to-one plots

The slopes of additional first-order (Table S1) and second-order (Table S2) FDM and HYD sensitivities comparisons are shown.

Table S1. Slope and R^2 of the comparisons of sensitivities of ground layer species concentrations to domain-wide perturbations

| Sensitivities: slope, R^2			
NO$_x$	SO$_2$	2nd-order NOx	2nd-order SO$_2$
$s_{NO_x}^{ANH_4}$: 0.99, 0.94	$s_{SO_2}^{ANH_4}$: 1.00, 0.97	$s_{NO_x}^{(2)ANH_4}$: 0.74, 0.67	$s_{SO_2}^{(2)ANH_4}$: 0.04, 0.04
$s_{NO_x}^{ANO_3}$: 1.00, 0.99	$s_{SO_2}^{ANO_3}$: 0.10, 0.30	$s_{NO_x}^{(2)ANO_3}$: 0.61, 0.38	$s_{SO_2}^{(2)ANO_3}$: 0.01, 0.00
$s_{NO_x}^{ASO_4}$: 1.00, 0.94	$s_{SO_2}^{ASO_4}$: 1.04, 1.00	$s_{NO_x}^{(2)ASO_4}$: 0.98, 0.96	$s_{SO_2}^{(2)ASO_4}$: 0.04, 0.06

Table S2. Slope and R^2 of the comparisons of ground layer species concentrations to domain-wide perturbations

| Sensitivities: slope, R^2			
TERP	APIN	2nd-order TERP	2nd-order APIN
s_{TERP}^{AMT1}: 1.00, 1.00	s_{APIN}^{AMT1}: 1.00, 1.00	$s_{TERP}^{(2)AMT1}$: 0.50, 0.49	$s_{APIN}^{(2)AMT1}$: 0.51, 0.50
s_{TERP}^{AMT2}: 1.00, 1.00	s_{APIN}^{AMT2}: 1.00, 1.00	$s_{TERP}^{(2)AMT2}$: 0.38, 0.38	$s_{APIN}^{(2)AMT2}$: 0.40, 0.39
s_{TERP}^{AMT3}: 1.01, 1.00	s_{APIN}^{AMT3}: 1.01, 1.00	$s_{TERP}^{(2)AMT3}$: 0.84, 0.72	$s_{APIN}^{(2)AMT3}$: 0.85, 0.74
s_{TERP}^{AMT4}: 1.01, 1.00	s_{APIN}^{AMT4}: 1.02, 1.00	$s_{TERP}^{(2)AMT4}$: 1.02, 0.94	$s_{APIN}^{(2)AMT4}$: 1.06, 0.94
s_{TERP}^{AMT5}: 1.02, 1.00	s_{APIN}^{AMT5}: 1.03, 1.00	$s_{TERP}^{(2)AMT5}$: 1.03, 0.95	$s_{APIN}^{(2)AMT5}$: 1.07, 0.95
s_{TERP}^{AMT6}: 1.02, 1.00	s_{APIN}^{AMT6}: 1.03, 1.00	$s_{TERP}^{(2)AMT6}$: 1.03, 0.95	$s_{APIN}^{(2)AMT6}$: 1.06, 0.95

Table S3. Individual module wall time of regular CMAQ (REG) and CMAQ-hyd (HYD) runs.

	HYD, 1 (s)	HYD, 2 (s)	HYD, 4 (s)	HYD, 8 (s)	REG, 1 (s)	REG, 2 (s)	REG, 4 (s)	REG, 8 (s)
Chem	5810	2930	1490	725	3180	1610	794	403
Aero	3840	1890	960	487	793	385	206	104
Vdiff	3860	1870	924	487	1390	724	393	217
Hadv	1270	757	474	320	589	334	216	160
Phot	462	205	124	64.0	235	111	53.4	28.9
Cldproc	301	173	94.8	56.9	149	81.4	41.3	27.4
Hdiff	221	141	83.0	56.9	70.6	47.1	29.1	23.1
Zadv	422	238	124	56.9	94.2	51.4	26.7	13.0
MPI_Barrier	2630	1830	1160	853	1160	796	561	368
Other	1290	778	492	448	188	137	107	99.6

3. Additional Figures
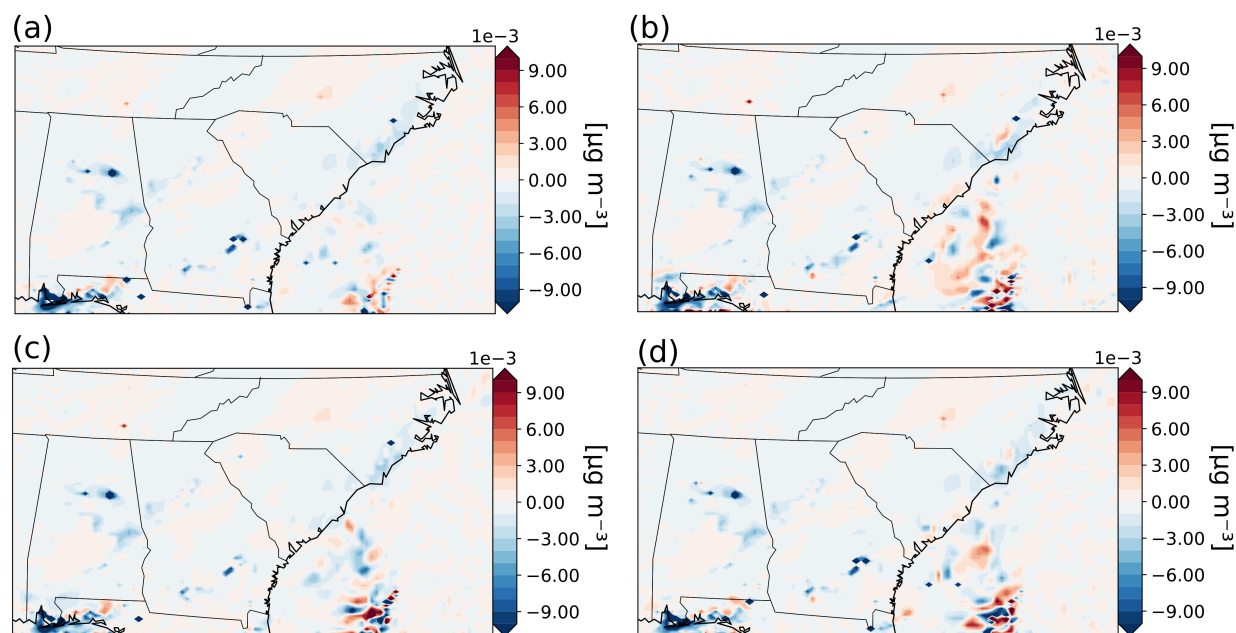
Figure S1. The first-order sensitivities of ground layer aerosol nitrate (ANO$_3$) concentration with respect to domain-wide perturbation of SO$_2$ emission calculated by FDM with different perturbation sizes: (a) 125%, 75%; (b) 110%, 90%; (c) 125%, 100%; (d) 100%, 75%. The sensitivities are apparently noisy, especially over the coast of South Carolina and Georgia.
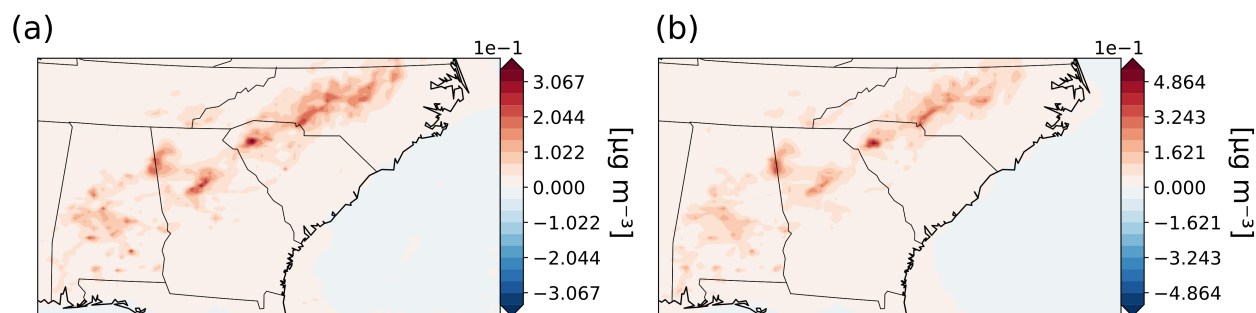
Figure S2. The first order sensitivities of (a): AMTNO$_3$ with respect to NOx, $s_{NO_x}^{AMTNO_3}$ and (b): AMTNO$_3$ with respect to monoterpenes, $s_{TERP}^{AMTNO_3}$

4. High-Performance Computing Clusters

The simulations were run on NCAR's Cheyenne Supercomputing Clusters (Computational Information Systems Laboratory, 2017). Cheyenne has 145,152 processor cores of 2.3 GHz Intel Xeon E5-2697V4 processors. The total system memory is 313 TB, with 64 GB per node on 3,168 nodes and 128 GB per node on 864 nodes. All the simulations in this work were run with 64 GB of memory per node.

References

Computational Information Systems Laboratory: Cheyenne: SGI ICE XA Cluster, 10.5065/D6RX99HX, 2017.
Fike, J. and Alonso, J.: The Development of Hyper-Dual Numbers for Exact Second-Derivative Calculations, 49th AIAA Aerospace Sciences Meeting including the New Horizons Forum and Aerospace Exposition, 2011-01-04, 10.2514/6.2011-886,